comparable than those shown in Figures 7–10. This is advantageous for WLAN operation, especially in indoor applications where the wave propagation is usually complex.

Figures 12 presents the measured antenna gain and simulated radiation efficiency. Figure 12(a) shows the results over the lower band for GSM operation. The antenna gain is varied from about 0.5–1.5 dBi, and the radiation efficiency is about 60–74%. For the results over the upper band for DCS/PCS/UMTS/WLAN operation, the antenna gain is varied from about 0.6–2.9 dBi, whereas the radiation efficiency is varied in the range of 62–88%.

4. CONCLUSION

A surface-mount multiband monopole slot chip antenna suitable for mobile phone application is presented. Different from the conventional monopole chip antenna using the metal strips as the resonant elements, which is usually not easy to achieve wide operating bandwidths, the proposed monopole slot chip antenna uses two monopole slots as the resonant elements and capable of generating a lower band at 900 MHz for GSM operation and an upper band for DCS/PCS/UMTS/WLAN operation. In addition, the antenna has a simple configuration and is easy to fabricate. It occupies a small area of 30×10 mm^2 on the system circuit board of the mobile phone, which can be further reduced to be 24×10 mm^2 only, when a ceramic base of relative permittivity 7.8 is used to replace the foam base, and the obtained bandwidth can still cover GSM/DCS/PCS/UMTS operation. Good radiation characteristics for frequencies over the antenna's lower and upper bands have also been obtained.

REFERENCES

1. Y.D. Kim and H.M. Lee, Design of compact triple-band meander chip antenna using LTCC technology for mobile handsets, Microwave Opt Technol Lett 48 (2006), 160–162.
2. Y.D. Kim, H.Y. Kim, and H.M. Lee, Dual-band LTCC chip antenna design using stacked meander patch for mobile handsets, Microwave Opt Technol Lett 45 (2005), 271–273.
3. D.S. Yim and S.O. Park, Small internal ceramic chip antenna for IMT-2000 handsets, Electron Lett 39 (2003), 1364–1365.
4. G.Y. Lee, H.T. Chen, and K.L. Wong, A low-cost surface-mount monopole antenna for GSM/DCS operation, Microwave Opt Technol Lett 37 (2003), 2–4.
5. K.L. Wong, S.W. Su, T.W. Chiou, and Y.C. Lin, Dual-band plastic chip antenna for GSM/DCS mobile phones, Microwave Opt Technol Lett 33 (2002), 330–332.
6. S.H. Sim, C.Y. Kang, S.J. Yoon, Y.J. Yoon, and H.J. Kim, Broadband multilayer ceramic chip antenna for handsets, Electron Lett 38 (2002), 205–207.
7. W. Choi, S. Kwon, and B. Lee, Ceramic chip antenna using meander conductor lines, Electron Lett 37 (2001), 933–934.
8. K.L. Wong, Planar antennas for wireless communications, Wiley, New York, 2003.
9. H. Wang, M. Zheng, and S.Q. Zhang, Monopole slot antenna, U.S. Patent No. 6,618,020 B2, (2003).
10. S.K. Sharma, L. Shafai, and N. Jacob, Investigation of wide-band microstrip slot antenna, IEEE Trans Antennas Propag 52 (2004), 865–872.
11. S.L. Latif, L. Shafai, and S.K. Sharma, Bandwidth enhancement and size reduction of microstrip slot antenna, IEEE Trans Antennas Propag 53 (2005), 994–1002.
12. A.P. Zhao and J. Rahola, Quarter-wavelength wideband slot antenna for 3–5 GHz mobile applications, IEEE Antennas Wireless Propag Lett 4 (2005), 421–424.
13. R. Bancroft, Dual slot radiating single feedpoint printed circuit board antenna, U.S. Patent No. 7,129,902 B2, (2006).
14. P. Lindberg, E. Ojefors, and A. Rydberg, Wideband slot antenna for low-profile hand-held terminal applications, Proc 36th European Microwave Conf (EuMC2006), Manchester UK, pp 1698–1701.
15. W.S. Chen and K.Y. Ku, Broadband design of a small non-symmetric ground $\lambda/4$ open slot antenna, Microwave J 50 (2007), 110–120.
16. C.I. Lin, K.L. Wong, and S.H. Yeh, Printed monopole slot antenna for multiband operation in the mobile phone, Proc 2007 IEEE AP-S Int Symp, Honolulu, Hawaii, USA, pp 629–632.
17. P.L. Sun, H.K. Dai, and C.H. Huang, Dual band slot antenna with single feed line, U.S. Patent No. 6,677,909 B2, (2004).
18. C.M. Su, H.T. Chen, and K.L. Wong, Inverted-L slot antenna for WLAN operation, Microwave Opt Technol Lett 37 (2003), 315–316.
19. C.M. Su, H.T. Chen, F.S. Chang, and K.L. Wong, Dual-band slot antenna for 2.4/5.2 GHz WLAN operation, Microwave Opt Technol Lett 35 (2002), 306–308.
20. K.L. Wong, Y.W. Chi, and S.Y. Tu, Internal multiband printed folded slot antenna for mobile phone application, Microwave Opt Technol Lett 49 (2007), 1833–1837.
21. C.M. Su, K.L. Wong, C.L. Tang, and S.H. Yeh, EMC internal patch antenna for UMTS operation in a mobile device, IEEE Trans Antennas Propag 53 (2005), 3836–3839.
22. S.L. Chien, F.R. Hsiao, Y.C. Lin, and K.L. Wong, Planar inverted-F antenna with a hollow shorting cylinder for mobile phone with an embedded camera, Microwave Opt Technol Lett 41 (2004), 418–419.
23. http://www.ansoft.com/products/hf/hfss/, Ansoft Corporation HFSS.
24. N. Behdad and K. Sarabandi, A multiresonant single-element wideband slot antenna, IEEE Antennas Wireless Propag Lett 3 (2004), 5–8.

INTERNAL MULTIBAND LOOP ANTENNA FOR GSM/DCS/PCS/UMTS OPERATION IN THE SMALL-SIZE MOBILE DEVICE

Chun-I Lin and Kin-Lu Wong
Department of Electrical Engineering, National Sun Yat-Sen University, Kaohsiung 804, Taiwan; Corresponding author: linci@ema.ee.nsysu.edu.tw

Received 16 September 2007

ABSTRACT: *An internal multiband loop antenna suitable for application in the small-size mobile device (groundplane length 50 mm only) is presented. Along the loop strip of the antenna, it is configured to have two symmetric meandered sections and a central widened section. With the configured loop strip, three resonant loop modes (0.5-, 1.0-, and 1.5-wavelength loop modes) can be excited to form two wide operating bands centered at about 900 and 1900 MHz for GSM/DCS/PCS/UMTS operation in the small-size mobile device. In addition, the loop antenna along with the short ground plane studied here shows near-omnidirectional radiation patterns in the azimuthal plane for frequencies over the antenna's two wide operating bands, which is different from conventional internal mobile phone antennas and is advantageous for practical applications.* © 2008 Wiley Periodicals, Inc. Microwave Opt Technol Lett 50: 1279–1285, 2008; Published online in Wiley InterScience (www.interscience.wiley.com). DOI 10.1002/mop.23337

Key words: *mobile antennas; loop antennas; internal mobile phone antennas; GSM/DCS/PCS/UMTS operation; multiband operation*

1. INTRODUCTION

Recently, with the rapid growth in mobile communications, multiband operation of the internal antennas for mobile devices such as the mobile phone, smart phone, and the like has become the basic requirement for practical applications. Many related designs of the internal planar inverted-F antenna (PIFA) for multiband operation

in the mobile phones have also been reported [1]. Such multiband internal PIFAs, however, are with unbalanced structures and will lead to large excited surface currents on the system ground plane. It is therefore well understood that the system ground plane of the mobile phone plays an important role in the performances of the internal PIFA, especially the antenna's achievable operating bandwidth [2]. Hence, it is usually difficult to obtain enough operating bandwidths for the internal PIFA to cover GSM/DCS operation, especially GSM operation in the 900-MHz band, when the system ground plane of the mobile phone has a length less than 80 mm.

In the recent studies, it has been demonstrated that the loop antennas are promising candidates for internal multiband operation in the mobile devices to excite relatively smaller surface currents on the system ground plane [3]. This attractive feature is mainly owing to the loop antenna operated as a balanced or quasi-balanced structure. In this case, the excited surface currents on the system ground plane can be greatly decreased, and hence the dependence of the antenna performances on the system ground plane can be relaxed. This suggests that the loop antennas are very promising for multiband operation in the mobile devices with a ground plane smaller than that of the conventional mobile devices. However, it is noted that the available internal multiband loop antennas that have been studied are with a system ground plane of length about 70 mm or larger [3–7].

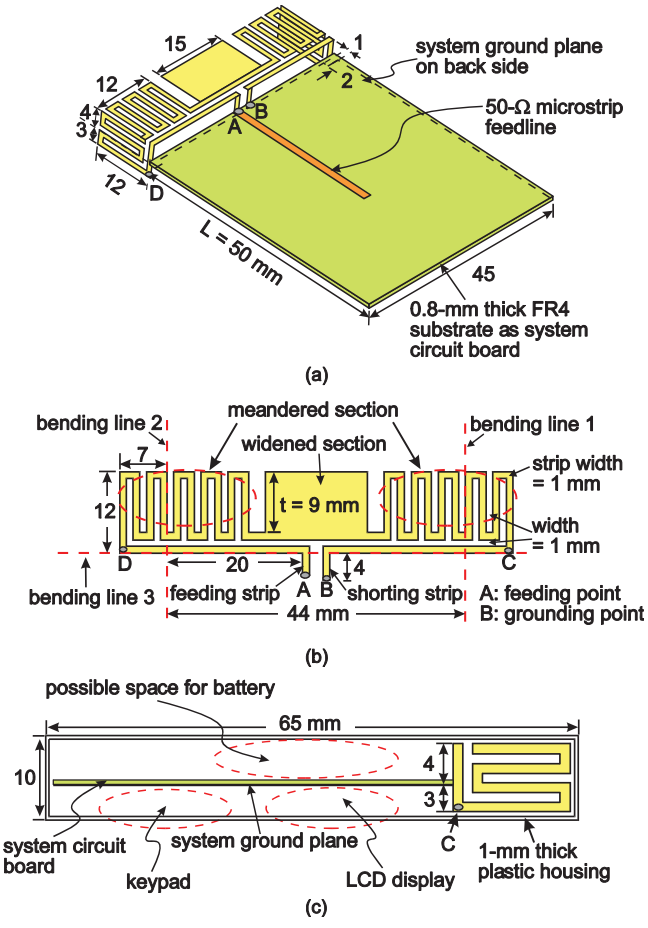

Figure 1 (a) Geometry of the proposed internal multiband loop antenna for application in the small-size mobile device. (b) Dimensions of the antenna unbent into the planar structure. (c) Side view of the antenna enclosed by a 1-mm thick plastic housing ($\varepsilon_r = 3.5$, $\sigma = 0.01$ S/m). [Color figure can be viewed in the online issue, which is available at www.interscience.wiley.com]

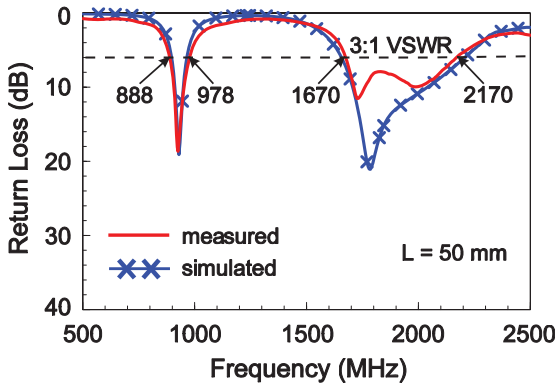

Figure 2 Measured and simulated return loss for the proposed antenna; the plastic housing is included. [Color figure can be viewed in the online issue, which is available at www.interscience.wiley.com]

In this study, we present a new design of the internal multiband loop antenna suitable for application in the mobile device with a small ground plane of length 50 mm only. The loop antenna can generate three resonant modes (0.5-, 1.0-, and 1.5-wavelength modes) to form two wide operating bands centered at about 900 and 1900 MHz to cover GSM (890–960 MHz), DCS (1710–1880 MHz), PCS (1850–1990 MHz), and UMTS (1920–2170 MHz) operation. In addition, the loop antenna has a simple configuration, allowing it to be easily fabricated from cutting a metal plate and then bending at its two side portions to achieve a compact size to be easily fit in the housing of the small-size mobile device with a thickness of 10 mm only. Geometry of the proposed multiband loop antenna is described, and design considerations of the antenna are presented. Effects of the major parameters on the antenna performances are also analyzed.

2. ANTENNA DESIGN

Figure 1(a) shows the geometry of the proposed internal multiband loop antenna applied in the small-size mobile device with a system ground plane of length 50 mm only. The system ground plane in this study is printed on a 0.8-mm thick FR4 substrate of size 45 × 50 mm^2, which is much smaller in length than that of the general mobile

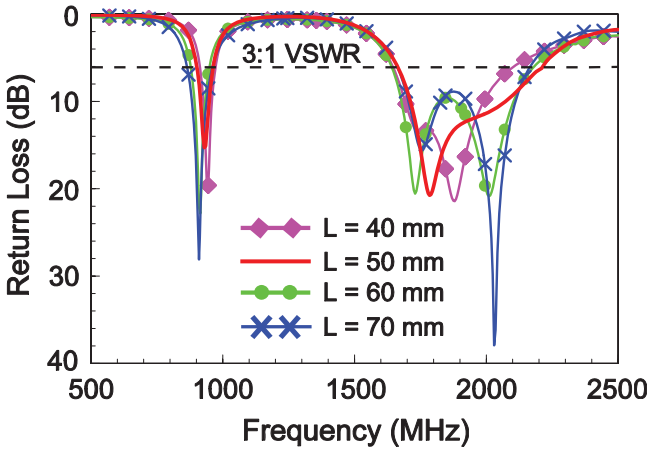

Figure 3 Simulated return loss as a function of the groundplane length L; other parameters are the same as studied in Figure 2. [Color figure can be viewed in the online issue, which is available at www.interscience.wiley.com]

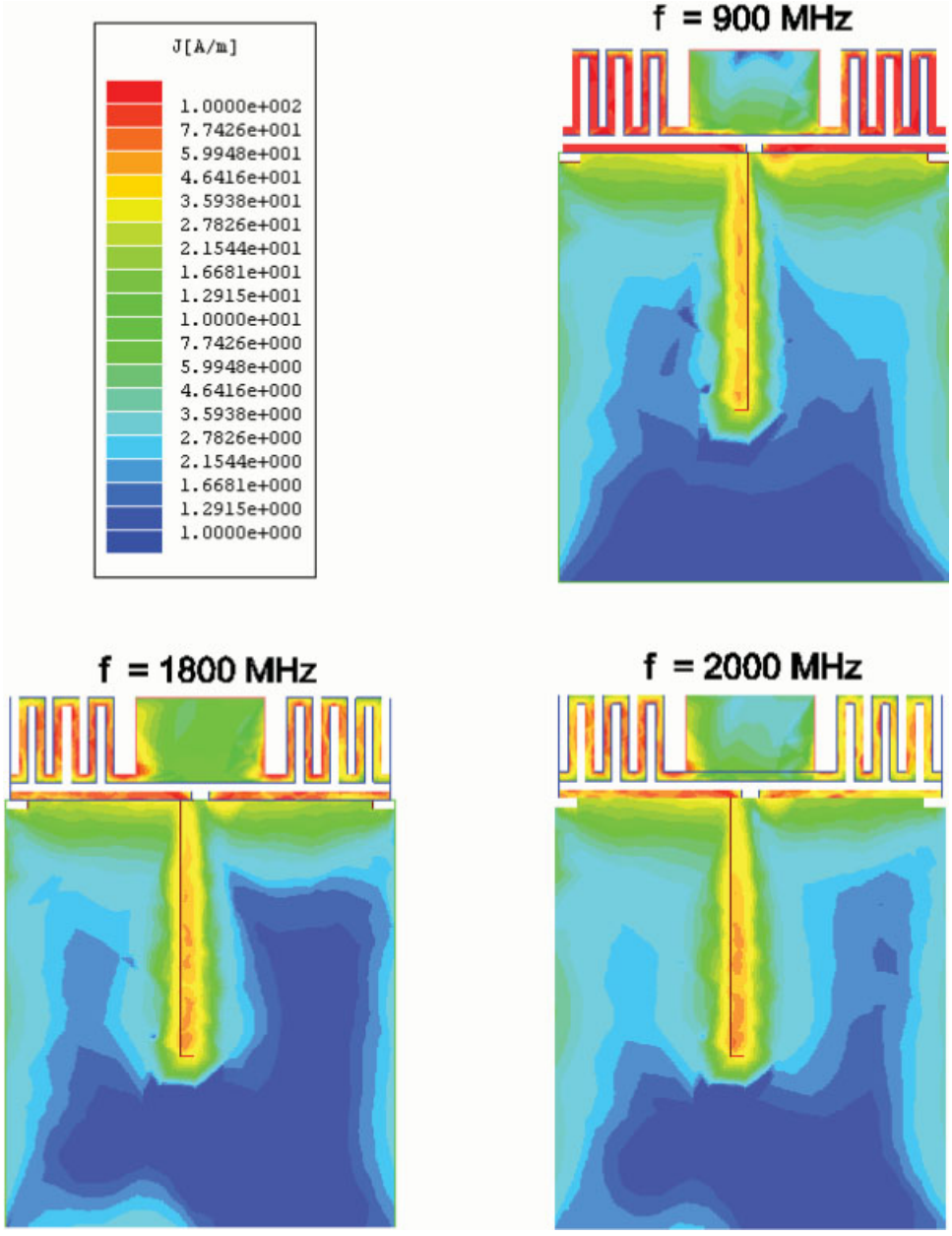

Figure 4 Simulated excited surface current distributions at 900, 1800, and 2000 MHz on the loop antenna and the system ground plane of length 50 mm studied in Figure 2. [Color figure can be viewed in the online issue, which is available at www.interscience.wiley.com]

phone. The antenna has a symmetric loop pattern, which is fabricated from line-cutting a 0.2-mm thick copper plate in the study. The loop pattern in its planar structure is shown in Figure 1(b). By bending the planar loop pattern at its two side portions (size 7 × 12 mm^2) by following bending lines 1 and 2, the loop antenna has a small thickness of 7 mm and hence can be easily fit in the housing of the thin mobile device of thickness 10 mm only [see Figure 1(c), the side view of the antenna enclosed by a 1-mm thick plastic housing of relative permittivity (ε_r) 3.5 and conductivity (σ) 0.01 S/m]. In Figure 1(c), the possible arrangement of the associated components such as the battery, display, and keypad are also shown.

By bending the third bending line, the loop pattern is connected at point A through the feeding strip of length 3.2 mm to the 50-Ω microstrip feedline printed on the front side of the system circuit board. The loop pattern is short-circuited to the ground plane on the back side of the system circuit board at point B through the shorting strip of length 4 mm. The distance between points A and B is 2 mm only. With the feeding point of the loop pattern located at about the centerline of the system circuit board, more symmetric radiation patterns for the proposed antenna can be obtained.

The loop pattern mainly comprises two symmetric meandered sections and a central widened section along the 1-mm wide loop strip. First note that the total length of the loop pattern is close to 0.5-wavelength at 900 MHz, which makes it possible for the loop antenna to generate a 0.5-wavlength mode at about 900 MHz (the antenna's lower band) to cover GSM operation. With the presence of the two meandered sections, the loop antenna can achieve a compact size. Furthermore, the meandered sections can effectively control the antenna's second and third resonant modes (1.0- and 1.5-wavelength modes) to occur at close frequencies to form a wide operating band (the antenna's upper band) to cover DCS/PCS/UMTS operation.

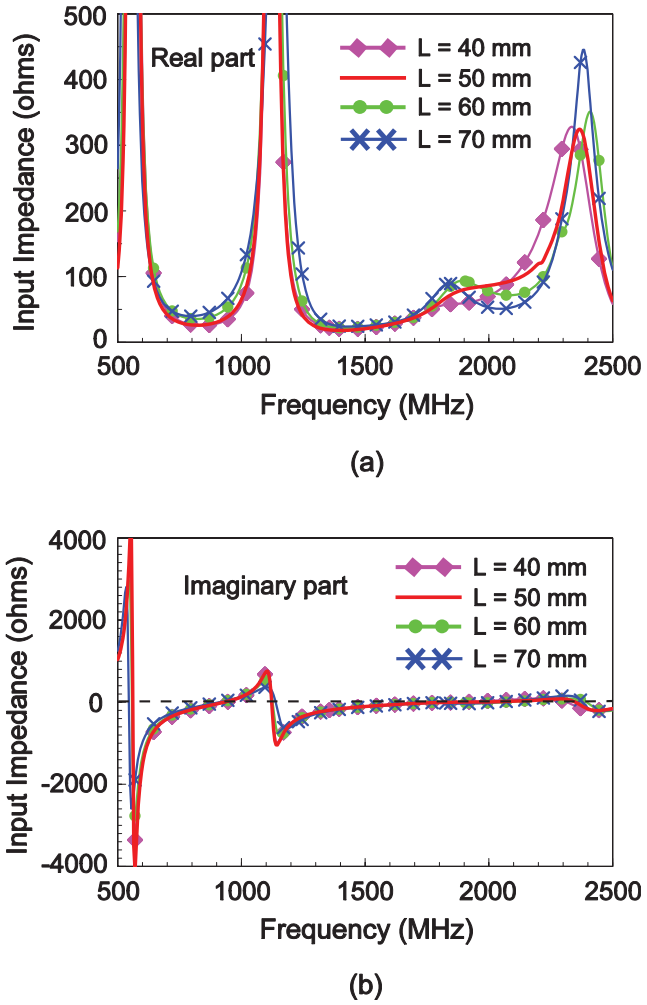

Figure 5 Simulated (a) real part and (b) imaginary part of the input impedance as a function of the groundplane length L; other parameters are the same as studied in Figure 2. [Color figure can be viewed in the online issue, which is available at www.interscience.wiley.com]

For the central widened section, it is chosen to have a width t of 9 mm and a length of 15 mm. With the widened section located at about the middle of the loop strip, fine-adjustment of the frequency ratio of the antenna's first three resonant modes (0.5-, 1.0-, and 1.5-wavelength modes) can be obtained. Enhanced impedance matching of the antenna's lower and upper bands can also be achieved. By incorporating the two meandered sections and the central widened section, the antenna's lower and upper bands can be tuned to be at about 900 and 1900 MHz to cover GSM/DCS/PCS/UMTS multiband operation. Effects of varying the width t of the widened section on the impedance matching of the antenna's three excited resonant modes are shown in Figure 6 for more detailed discussion in the next section. Also note that there are two small notches of size 2×1 mm^2 on the top two corners of the system ground plane, which are used to avoid the two bending portions of the antenna contacting with the system ground plane.

3. RESULTS AND DISCUSSION

On the basis of the design dimensions given in Figure 1, the antenna was fabricated and tested. Figure 2 shows the measured and simulated return loss of the fabricated prototype enclosed by the plastic housing shown in Figure 1(c). The simulated results are obtained using Ansoft HFSS [8], and good agreement between the simulation and measurement is obtained. Three resonant modes at about 900, 1800, and 2000 MHz are successfully excited. From the measured results, the antenna's lower band formed by the first resonant mode has a bandwidth of 90 MHz (888–978 MHz), which covers GSM operation. The antenna's upper band formed by the second and third resonant modes shows a large bandwidth of 500 MHz (1670–2170 MHz), which covers DCS/PCS/UMTS operation. Note that the bandwidth definition is 3:1 VSWR (6-dB return loss), which is generally selected as the internal mobile phone antenna design specification.

Effects of the groundplane length L on the antenna performances are also analyzed. Figure 3 shows the simulated return loss for the cases with L varied from 40 to 70 mm. It is seen that the obtained bandwidth for the antenna's lower band at about 900 MHz is increased when the length L increases. For the upper band at about 1900 MHz, the obtained bandwidths for the length L = 50, 60, and 70 mm are about the same. For L = 40 mm, the upper-band bandwidth is decreased; however, it can still cover DCS/PCS operation. In general, the variations in the obtained bandwidths of the lower and upper bands for the proposed loop antenna are smaller than those observed for the conventional internal multiband PIFAs [9, 10].

Figure 4 shows the excited surface current distributions at 900, 1800, and 2000 MHz for the 0.5-, 1.0-, and 1.5-wavelength modes on the loop antenna and the system ground plane of length 50 mm studied in Figure 2. For other frequencies over the three excited resonant modes, the obtained surface current distributions are about the same as shown here. It is seen that because of the balanced characteristic of the 1.0-wavelength mode, there are small excited surface currents on the system ground plane at 1800 MHz. It is interesting to find that the excited surface current distributions on the system ground plane at 900 and 2000 MHz are similar to that at 1800 MHz, indicating that the 0.5- and 1.5-wavelength modes also show similar balanced characteristic. In addition, there are no nulls in the excited surface currents, except at the region near the lower edge of the system ground plane. This makes it possible for the antenna to achieve omnidirectional or near-omnidirectional radiation in the azimuthal plane. Related radiation characteristics will be discussed later in this section.

Figure 5 shows the real and imaginary parts of the input impedance of the antenna for the cases with L = 40, 50, 60, and

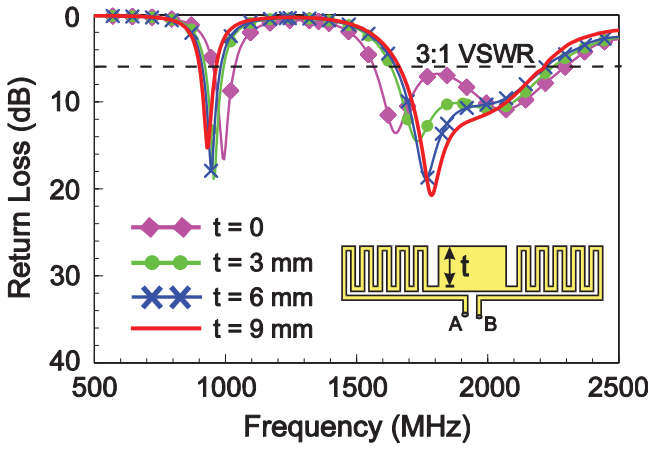

Figure 6 Simulated return loss as a function of t, width of the central widened section; other parameters are the same as studied in Figure 2. [Color figure can be viewed in the online issue, which is available at www.interscience.wiley.com]

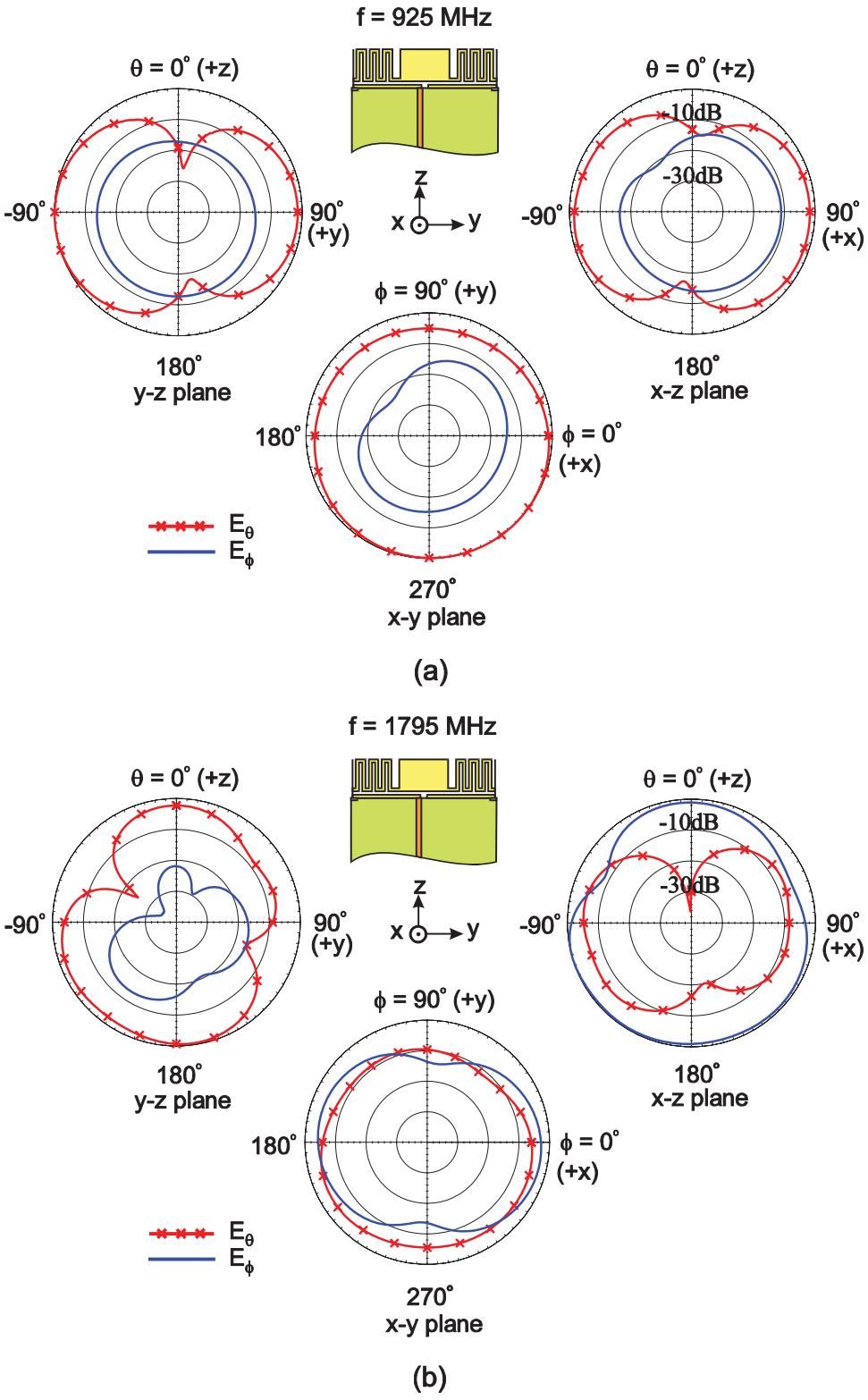

Figure 7 Measured radiation patterns at (a) 925 MHz and (b) 1795 MHz for the antenna studied in Figure 2. [Color figure can be viewed in the online issue, which is available at www.interscience.wiley.com]

70 mm. Results show that, when the length L is decreased from 70 to 40 mm, the variations of the input impedance for the antenna operating in the lower band at about 900 MHz and the upper band centered at about 1900 MHz are generally small. This behavior also explains the bandwidth variations shown in Figure 3 and makes the proposed antenna suitable for application in the small-size mobile device.

Figure 6 shows the effects of the central widened section on adjusting the three excited resonant modes to form the antenna's lower and upper bands for multiband operation. It is seen that, with an increase in the width t of the central widened section, the first resonant mode is shifted to lower frequencies, and the second and third resonant modes are shifted to be closer to each other. For the case with $t = 9$ mm (the preferred dimensions shown in Fig. 1), the

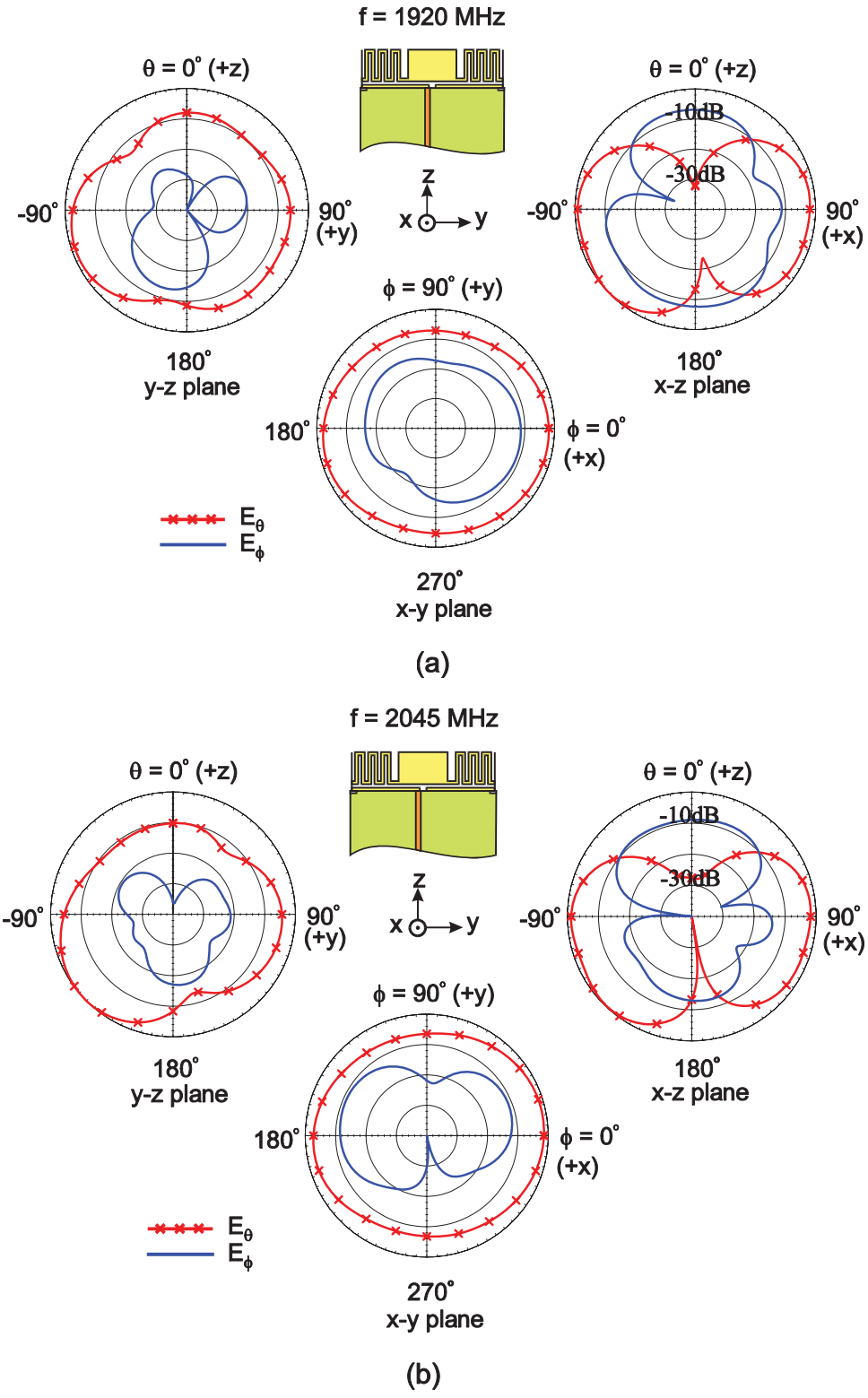

Figure 8 Measured radiation patterns at (a) 1920 MHz and (b) 2045 MHz for the antenna studied in Figure 2. [Color figure can be viewed in the online issue, which is available at www.interscience.wiley.com]

first resonant mode is adjusted to be at about 900 MHz to cover GSM operation, and the upper band formed by the second and third resonant modes is centered at about 1900 MHz to cover DCS/PCS/UMTS operation.

Figures 7 and 8 plot the measured radiation patterns at 925, 1795, 1920, and 2045 MHz (center frequencies of the GSM, DCS, PCS, and UMTS bands) for the antenna studied in Figure 2. For operating at 925 MHz, monopole-like radiation patterns are seen with near-omnidirectional radiation in the azimuthal plane (x–y plane) [see Fig. 7(a)], which is similar to those of the conventional internal mobile phone antennas [1]. For operating in the upper band [see 1795 MHz in Fig. 7(b), 1920 MHz in Fig. 8(a), and 2045

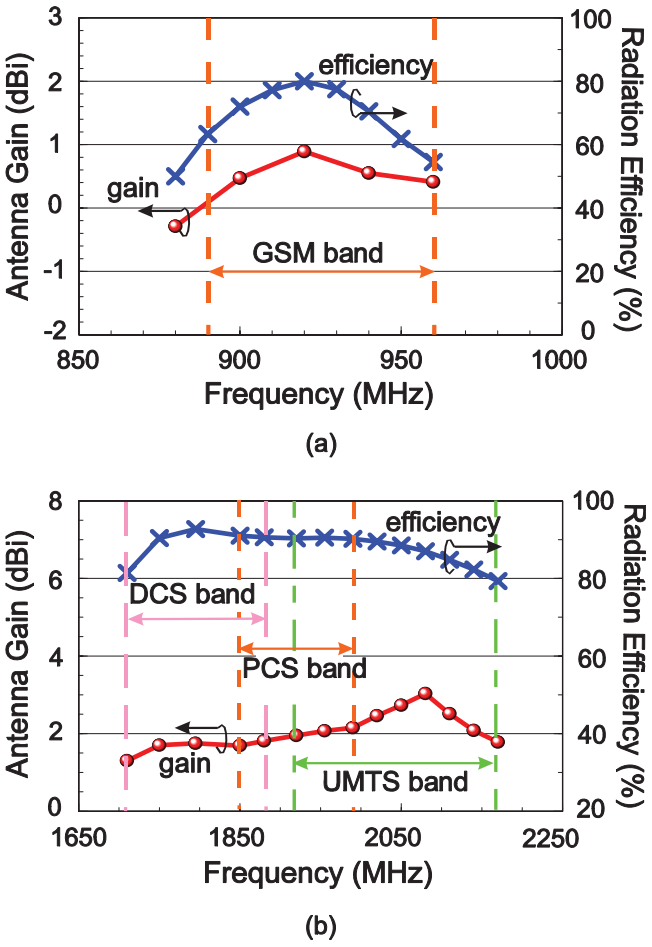

Figure 9 Measured antenna gain and simulated radiation efficiency of the antenna studied in Figure 2. (a) The lower band for GSM operation. (b) The upper band for DCS/PCS/UMTS operation. [Color figure can be viewed in the online issue, which is available at www.interscience.wiley.com]

MHz in Fig. 8(b)], near-omnidirectional radiation in the azimuthal plane is also seen, which is advantageous for practical applications and, however, is quite different from that observed for the conventional internal mobile phone antenna with the system ground plane of length larger than 80 mm [1]. One possible reason is that the second and third resonant modes of the proposed loop antenna generally show similar balanced characteristic, which results in smaller excited surface currents on the system ground plane. Another reason is that, for the ground plane with a smaller length, the nulls in the excited surface currents for frequencies over the upper band centered at about 1900 MHz will be located closer to or at the lower edge of the ground plane. These reasons make the radiation patterns for frequencies over the upper band show near-omnidirectional characteristic.

Measured antenna gain and simulated radiation efficiency are presented in Figure 9. For frequencies over the GSM band shown in Figure 9(a), the antenna gain is varied from about 0.1 to 0.9 dBi and the radiation efficiency is all larger than 55%. For frequencies over the DCS/PCS/UMTS bands, the antenna gain is varied from about 1.3 to 3.0 dBi and the radiation efficiency is all larger than about 80%. The obtained results indicate that good radiation characteristics are obtained for the proposed loop antenna.

4. CONCLUSION

An internal multiband loop antenna capable of GSM/DCS/PCS/UMTS operation for applying in the small-size mobile device has been proposed and studied. Three resonant modes (0.5-, 1.0-, and 1.5-wavelength modes) with similar balanced characteristic have been obtained, which are formed into two wide operating bands for the proposed antenna to cover multiband operation. In addition, good radiation characteristics with near-omnidirectional radiation patterns in the azimuthal plane of the mobile device for frequencies over the antenna's lower and upper bands have been obtained, which are advantageous and attractive for practical applications.

REFERENCES

1. K.L. Wong, Planar antennas for wireless communications, Wiley, New York, 2003, Chapter 2.
2. T.Y. Wu and K.L. Wong, On the impedance bandwidth of a planar inverted-F antenna for mobile handsets, Microwave Opt Technol Lett 32 (2002), 249–251.
3. Y.W. Chi and K.L. Wong, Internal compact dual-band printed loop antenna for mobile phone application, IEEE Trans Antennas Propagat 55 (2007), 1457–1462.
4. C.I. Lin and K.L. Wong, Internal meandered loop antenna for GSM/DCS/PCS multiband operation in a mobile phone with the user's hand, Microwave Opt Technol Lett 49 (2007), 759–765.
5. W.Y. Li and K.L. Wong, Surface-mount loop antenna for AMPS/GSM/DCS/ PCS operation in the PDA phone, Microwave Opt Technol Lett 49 (2007), 2250–2254.
6. B. Jung, H. Rhyu, Y.J. Lee, F.J. Harackiewwicz, M.J. Park, and B. Lee, Internal folded loop antenna with tuning notches for GSM/GPS/DCS/PCS mobile handset applications, Microwave Opt Technol Lett 48 (2006), 1501–1504.
7. B.K. Yu, B. Jung, H.J. Lee, F.J. Harackiewwicz, and B. Lee, A folded and bent internal loop antenna for GSM/DCS/PCS operation of mobile handset applications, Microwave Opt Technol Lett 48 (2006), 463–467.
8. Ansoft Corporation HFSS, available at http://www.ansoft.com/products/hf/hfss/.
9. K.L. Wong, Y.C. Lin, and T.C. Tseng, Thin internal GSM/DCS patch antenna for a portable mobile terminal, IEEE Trans Antennas Propagat 54 (2006), 238–242.
10. O. Kivekas, J. Ollikainen, T. Lehtiniemi, and P. Vainikainen, Bandwidth, SAR, and efficiency of internal mobile phone antennas, IEEE Trans Antennas Propagat 46 (2004), 71–86.

MODIFIED CIRCULAR MONOPOLE ANTENNA WITH IMPROVED TRANSMISSION PERFORMANCE FOR UWB COMMUNICATIONS

Qi Wu, Ronghong Jin, and Junping Geng
Department of Electronic Engineering, Shanghai Jiao Tong University, Shanghai 200240, China; Corresponding author: wuqi2004@sjtu.edu.cn

Received 17 September 2007

ABSTRACT: *This study theoretically analyses the transmission performance of UWB antennas and presents a design methodology for improving the transmission performance of printed monopoles. Using this methodology, a modified circular monopole are proposed and analyzed as the design example. Both measured and simulated results are provided and discussed for verifying the validity of proposed design methodology. In a typical lab environment, the deleterious multi-path transmission effects on the transfer function of the example antenna pair were observed and discussed. This optimization methodology would not bring any size or cost increase to the printed monopoles, and the improvement of transmission performance is quite discernible, which appears to be a significant improvement over printed UWB mono-*